

CRYSTAL STRUCTURE, SURFACE ACIDITY, SURFACE AREA, CATALYTIC ACTIVITY AND ELECTRICAL CONDUCTIVITY BEHAVIOUR OF $\text{SiO}_2\text{-ZrO}_2$ SYSTEM

Z.A. OMRAN

Chemistry Department, Faculty of Science, Zagazig University, Benha Branch.

(Received Nov. 8, 1993; Revised June 16, 1994; Accepted June 27, 1994)

SUMMARY

Crystal structure, surface acidity, surface area, catalytic activity and electrical conductivity behaviour of $\text{SiO}_2\text{-ZrO}_2$ system of various composition has been investigated. Samples with 50 % ZrO_2 calcined at 550, 650 and 750°C showed a high concentration of acidic sites and catalytic activity for the H_2O_2 decomposition. The electrical conductivity of $\text{SiO}_2\text{-ZrO}_2$ mixture calcined at 750°C showed a lower value than the pure ZrO_2 . The results obtained have been discussed and correlated.

1- INTRODUCTION

The amorphous silica of commercial importance have a high surface area (100-500 m^2/g) and find industrial use as adsorbents, catalysts, supports, and filters for paints, toothpaste, etc. Intrusion of ZrO_2 in the mixed $\text{SiO}_2 \cdot x \text{H}_2\text{O-ZrO}_2$ systems forming crystal defects which causes a change in the physical and chemical characteristics, especially their acidity and their electrical conductivity (1-7).

Many types of defects can be present in the texture of the crystal lattice of solids. Surface defects have different energy and structure from that of the bulk of the solid. These effects indicate that the material gains certain physical properties such as catalytic activity due to these defects(8).

There are a number of reports concerning the acid properties of solid catalyst and the correlation between catalytic activity and surface acidity. ZnO-TiO_2 was most extensively studied(9) and recently some other mixed metal oxides were also studied Silica-zirconia(10) and Silica-Magnesia(11) were reported to be solid acid which can act a cracking catalysts. Kawaguchi and Haregawa studied(12) the surface acidity $\text{SiO}_2\text{-TiO}_2$ catalysts with variuos amounts of TiO_2 content. They found

that the highest acid amount and acid strength for a molar ratio of 1:1. The acid amount were 0.34, 0.57 and 0.65 mmol/g at $H_o = -8.2$, -5.6 , -3.0 and $+4.0$ respectively. From the previous works, (13–15) decomposition of H_2O_2 and the acidic properties of some inorganic solids showed a good correlation between the acidic and the catalytic properties.

The present work was designed to measure the acidity of the binary metal oxides. ZrO_2-SiO_2 , with *n*-butylamine and benzoic acid respectively, using various indicator of $pK_a = -8.8$ to -3.3 . Effects of the chemical composition and the crystal structure on the acid properties were also studied. The electrical conductivity and the catalytic decomposition of H_2O_2 by these catalysts have been studied.

2- EXPERIMENTAL

The binary oxides $SiO_2 \cdot x H_2O - ZrO_2$ were prepared in the composition 10:90, 20:80, 40:60, 50:50, 70:30 and 90:10 mole % of $ZrO_2 - SiO_2 \cdot x H_2O$ respectively, from BDH quality chemicals by impregnation technique. The samples are designated as sample I, II, III, IV, IV, V and VI respectively. The impregnated oxides were dried at $115^\circ C$ for 5 hours. The samples were then ground and only such samples collected between 100 and 200 mesh series were used. The powders, thus obtained were calcined at 550, 650 and $800^\circ C$ for 5 hours at each of these temperature. The samples after calcination were cooled in a desiccator and kept in covered glass tubes under vacuum.

X-ray diffraction patterns of the samples investigated by the aid of Philips diffractometer, type Pw 2103/100 using Cu-target and Ni-filter.

IR absorption spectra on the samples were carried out with Beckman infrared spectrophotometric, unit, adopting KBr technique.

DTA and TGA experiments were carried out using a Shimadzu Thermal Analyzer (model 30) at heating rate $20^\circ C \text{ min}^{-1}$ in air atmosphere using 20 mg Sample.

Surface area on the samples were carried out using the nitrogen adsorption technique. Adsorption-desorption isotherms were obtained for each sample from the adsorption of nitrogen gas at liquid nitrogen temperature (77.2 K). Each sample was outgassed for 5 hours at $110^\circ C$ prior to any adsorption run.

The acidic sites for the pure and mixed oxides surface were determined by using the amine titration method developed by Johnson. (16) So 0.2g of the sample suspended in benzene was titrated with a solution of 0.1N n-butylamine in benzene using anthraquinone ($\text{pK}_a = -8.2$), benzal acetophenone ($\text{pK}_a = -5.6$), dicinimal actone ($\text{pK}_a = -3.0$), as indicators. The decomposition of H_2O_2 was selected for the study on catalytic reactivity of the catalysts (17) in a temperature range 30–50°C. The electrical conductivity has been measured by a method was reported elsewhere.(18)

3- RESULTS AND DISCUSSION

Figures (1, 2) represent the DTA and TG diagrams respectively for $\text{SiO}_2 \cdot x\text{H}_2\text{O}$, ZrO_2 and $\text{SiO}_2 \cdot x\text{H}_2\text{O} - \text{ZrO}_2$ mixtures. The TG diagrams of silica gel shows continuous decrease in weight at a temperature range of 30–1200°C whereas the DTA diagram shows two endothermic peaks at 70 and 600°C. The first small peak appearing at 70°C may be attributed to the desorption of H_2O molecules from the surface of the oxide while the second peak appearing at 600°C is explained on the basis of the transformation of silica gel to SiO_2 . This transformation was also studied by other authors. (19–23)

The DTA–TG diagram of the impregnated ZrO_2 , Fig. (1) showed endothermic peak at 150°C with a decreasing in the weight (3.2 %) due to the elemination of lousy bonded water molecules and a broad exothermic peak around 480°C which attributed to the crystallization of zirconia.

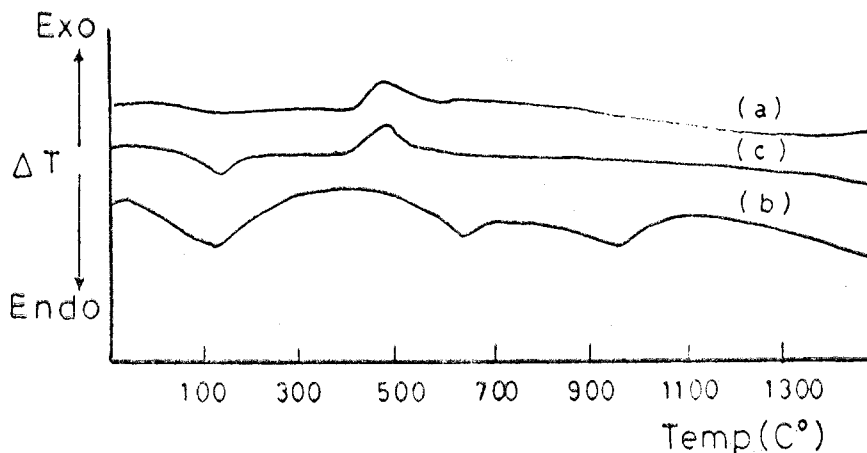


Fig. 1. DTA Curves of (a) Zirconia, (b) Silica gel and (c) Silica gel-Zirconia Mixture.

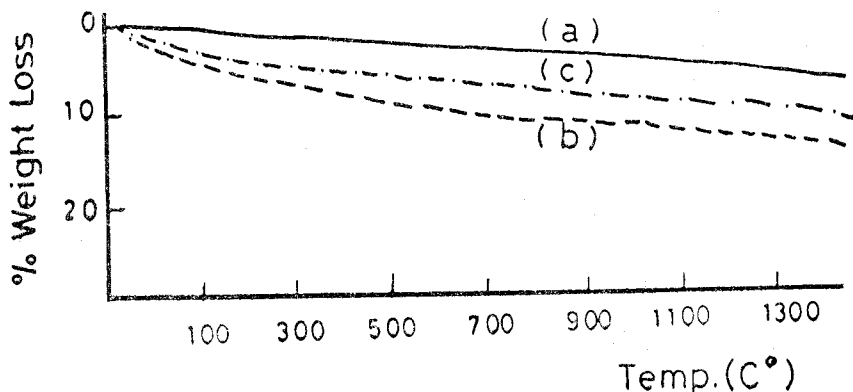


Fig. 2. TGA Curves of (a) Zirconia, (b) Silica gel and (c) Silica gel-Zirconia Mixture.

The DTA-TG diagrams $\text{SiO}_2 \cdot x \text{H}_2\text{O} - \text{ZrO}_2$ mixture (1:1 molar ratio) showed only the same peaks characteristic for the pure oxides, which means that no chemical reaction occurs between the two oxides in the investigated temperature range.

Figure (3) shows the IR spectra of $\text{SiO}_2 \cdot x \text{H}_2\text{O}$ and ZrO_2 and their mixtures with (1:1 molar ratio). The IR spectra for silica gel samples shows 4 bands at 800, 1100, 1650 and 3400 cm^{-1} . The first 2 bands are assigned to Si-O vibrations. (24, 25) The last two bands is assigned to Si...OH and H...O...H binding vibration. On the other hand, the IR spectra of ZrO_2 show two band at 740 and 3400 cm^{-1} due to Zr-O and H...O...H binding vibration. The IR spectra of oxide mixtures show a modification in the bands of the SiO_2 catalyst by ZrO_2 lead to a significant change. The addition of 10, 20 and 40 mole % ZrO_2 to SiO_2 causes a change in the sharp absorption band at 800°C to a broad band and the appear of new band from 730 to 780 cm^{-1} . This modification in the vibration bands are increased by increasing the percentage of ZrO_2 in the oxide mixture. This shift can be attributed to the presence of Zr^{+4} in sites near to the Si-O vibrating band.

Fig. (4) shows the X-ray diffraction patterns for calcined pure and mixed oxides (1:1 molar ratio of the products of thermal treatment of $\text{SiO}_2 \cdot x \text{H}_2\text{O}$ and ZrO_2 at different calcination temperature. All calcined samples of ZrO_2 and its mixtures with silica gel showed the same diffraction lines, which are characteristic for monoclinic ZrO_2 structure. The absence of new X-ray diffraction lines for the investigated product

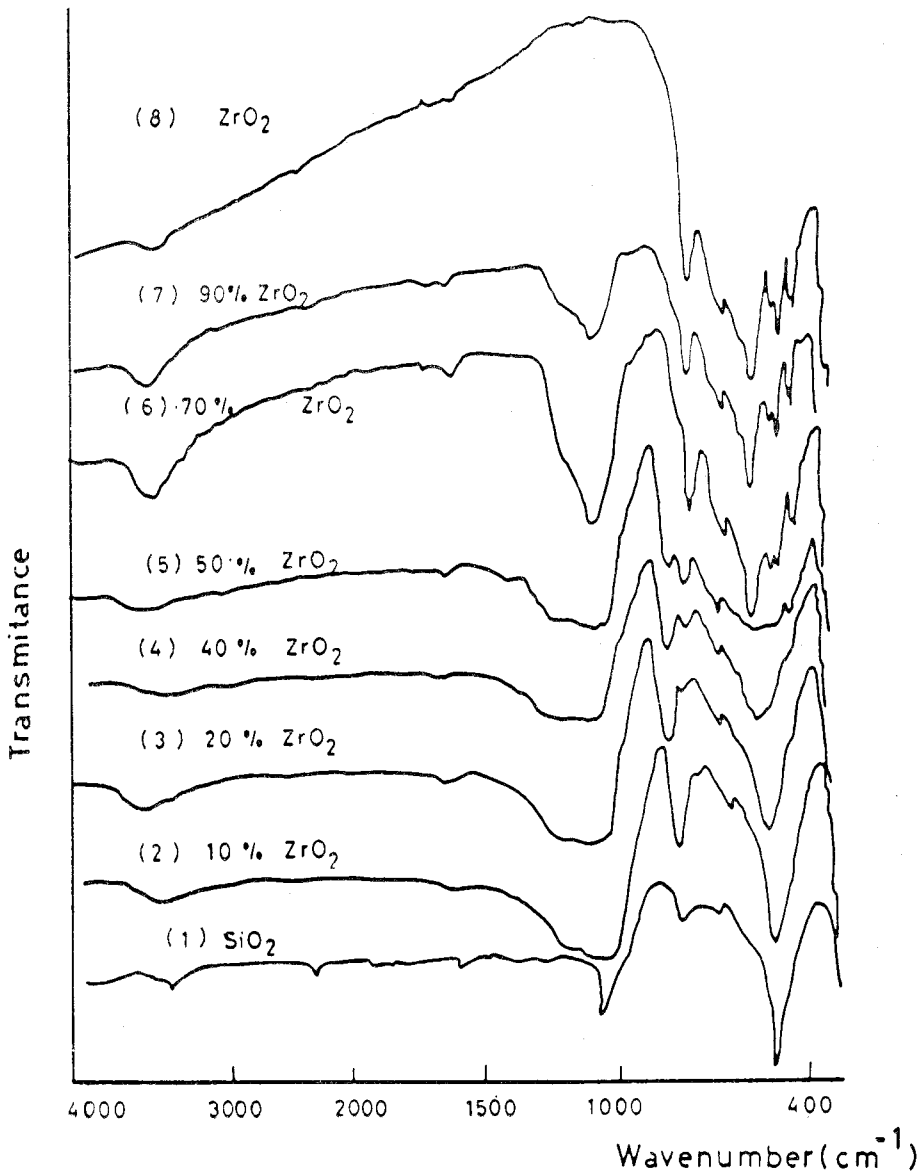


Fig. 3. IR Absorption Spectra of $\text{ZrO}_2\text{-SiO}_2\text{xHO}$ Mixtures with Different Mole Ratios.

indicates that no reaction has occurred between ZrO_2 and $\text{SiO}_2 \cdot x \text{H}_2\text{O}$ at the investigated calcination temperature (550, 650 and 800°C).

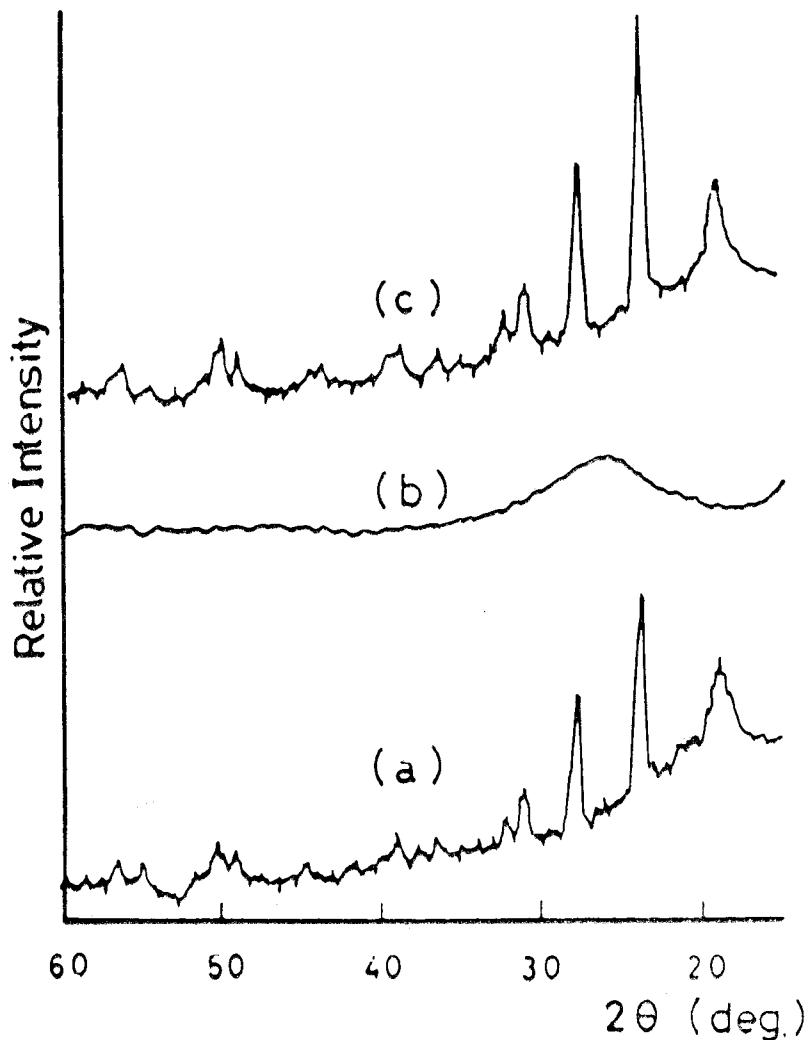


Fig. 4. X ray Diffraction Patterns for (a) $\text{SiO}_2 + \text{ZrO}_2$ Calcined at 850°C, (b) SiO_2 Calcined at 850°C, (c) ZrO_2 Calcined at 850°C.

From Fig. (5a) non linear behaviour between the acidity and the composition of the oxides can be observed. Maximum acid amount at any acid strength and different calcination temperature were observed

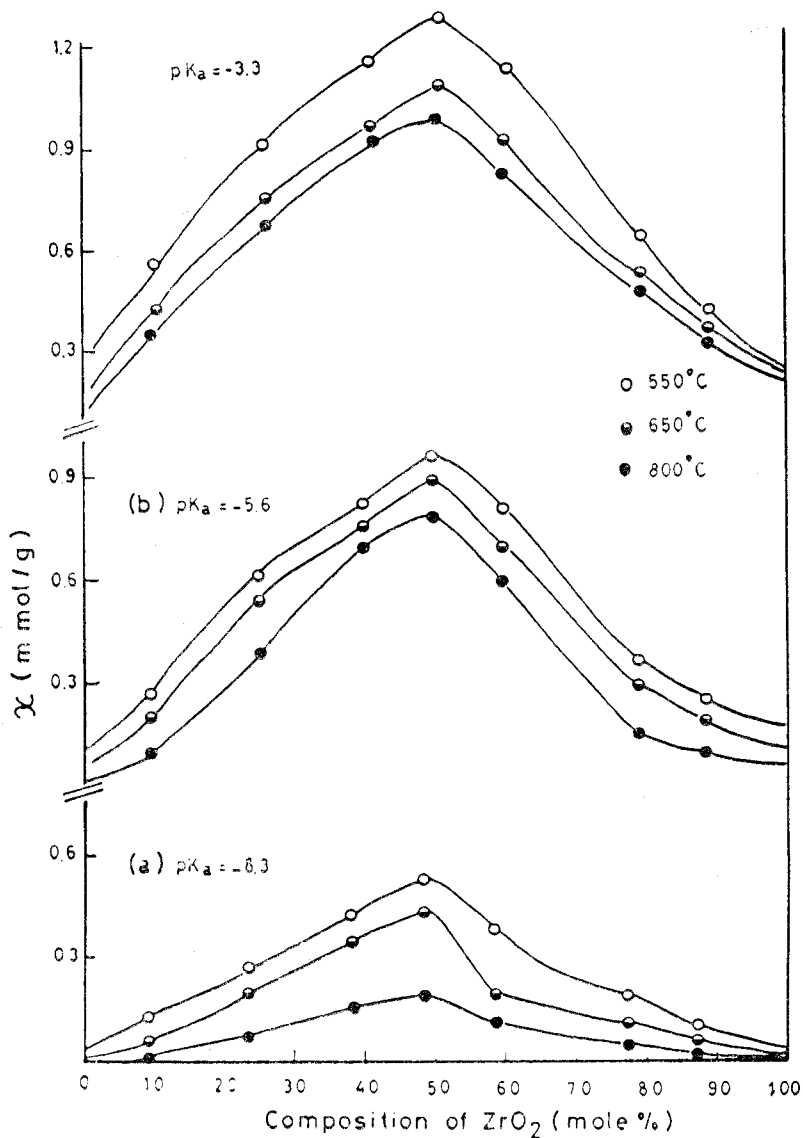


Fig. 5. The Variation of Acidity (Expressed as m. mol. of n. butylamine/g of Catalyst) With The Composition and Calcination Temp.

for sample with the molar ratio 1:1 Moreover the number of acid sites was found to be decreases with increasing calcination temperature for all samples investigated. Fig. (6) shows a linear correlation between the acidity and the calcination temperature for each investigated com-

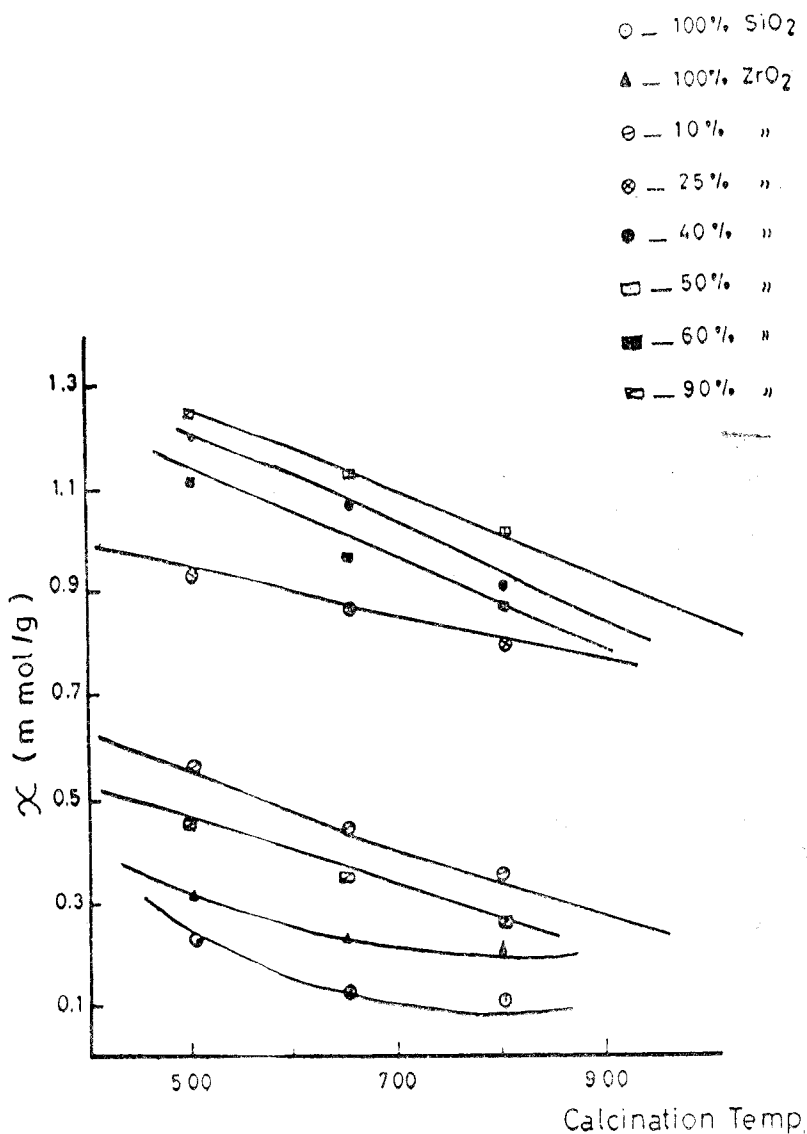


Fig. 6. Effect of Calcination Temperature on The Acidity of SiO₂-ZrO₂ at Various Compositions.

position. This indicates that the decrease in acidity of $\text{SiO}_2\text{-ZrO}_2$ with the heat treatment due to the decrease in the number of acid sites rather than to the change in their nature of the $\text{SiO}_2\text{-ZrO}_2$ system. The acidity at various strength of the catalysts are shown in the Figure (5). The maximum acidities at $\text{pK}_a = -3.3, -5.6$ and -8.3 observed for $\text{SiO}_2\text{-ZrO}_2$ of mole ratio 1:1 where higher than the acidity of $\text{SiO}_2\text{-TiO}_2, \text{SiO}_2\text{-ZnO}$ and $\text{SiO}_2\text{-Al}_2\text{O}_3$. The all ratios for $\text{SiO}_2\text{-ZrO}_2$ changed even the basic colours of acid indicators. Specific surface areas of the catalysts calcined at 550 and 650°C were determined in Table (1). It shows that the specific surface areas for $\text{SiO}_2\text{-ZrO}_2$ system increases with increasing ZrO_2 ratio up to 50 % and then decreases again up to 100 % ZrO_2 . This means that the change in acidic property by mixing each oxide is partly due to the change in surface area, but the acidities per unit surface area of $\text{SiO}_2\text{-ZrO}_2$ are much larger than those of single oxides.

Table 1. Specific surfaces area for calcined samples at different temperatures.

Composition samples	$A_1, \text{m}^2/\text{g}$	$A_2, \text{m}^2/\text{g}$
SiO_2	160	132
I	190	184
II	220	185
III	245	215
IV	270	230
V	220	170
VI	185	165
ZrO_2	62	48

A_1 : For the samples were calcined at 550°C.

A_2 : For the samples were calcined at 650°C.

The specific rate constants, k , for the catalyzed decomposition of H_2O_2 on $\text{SiO}_2\text{-ZrO}_2$ system are shown in Table (2). From which it can be seen that the rate of the decomposition of H_2O_2 changes with the composition of oxides, a typical plot is given in Fig. (7). Similar behaviours were observed for each of the calcination temperatures. The k -values decrease with increasing calcination temperatures in the order $k_{500} > k_{600} > k_{800}$. The effect of calcination temperatures on the reactivity of the oxides follows the same trend observed for the acidity results, where the number of acidic sites on the oxides at 800°C are lower than those obtained at lower calcination temperatures. From Fig. (7) it can also be seen that the rate of H_2O_2 decomposition increases first with increasing the concentration of ZrO_2 to a maximum at 50 mole % ZrO_2 , then decreases to a minimum at 100 mole % ZrO_2 .

Table 2. Kinetic Data (at 50 °C) of the catalytic decomposition of H₂O₂ over different composition of ZrO₂-SiO₂ System.

Calcination Temperature (°C)	550 °C			650 °C			750 °C		
	kx 10 ⁻⁵ (S ⁻¹)	E (kimol ⁻¹)	r	kx 10 ⁻⁶ (S ⁻¹)	E (kimol ⁻¹)	r	kx 10 ⁻⁷ (S ⁻¹)	E (kijmol ⁻¹)	r
I	1.126	53.531	0.975	0.800	100.02	0.992	2.097	116.0511	0.9
II	5.257	84.08	0.980	4.58	80.60	0.984	3.918	120.9541	0.9
III	7.0928	68.035	0.905	7.656	52.340	0.981	5.89	80.8461	0.9
IV	8.489	24.671	0.999	21.543	68.69	0.884	6.96	72.4730	0.9
V	7.156	42.6455	0.991	5.242	24.360	0.998	3.651	64.8541	0.9
VI	5.6015	36.820	0.994	2.215	36.441	0.999	2.15	48.935	0.9
ZrO ₂	7.610	32.707	0.999	0.5089	61.27	0.986	1.45	52.736	0.9

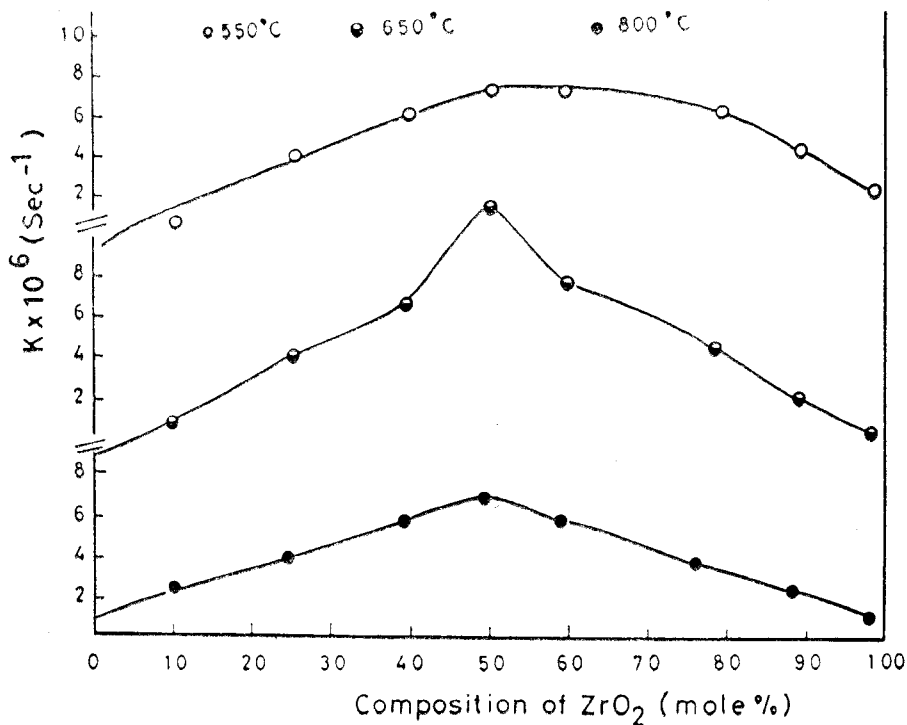
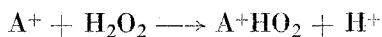


Fig. 7. Effect of Composition and Calcination Temperature on The Decomposition Rate of H₂O₂.

By comparing the reactivity results with those obtained for acidity (maximum at 50 mole % ZrO_2), it can be seen that the decomposition of H_2O_2 over the oxides with different concentration is attributed to the acidic sites present on the surfaces. On the other hand, the reactivity of the oxides containing lower or higher concentration (less or higher than 50 mole % ZrO_2) can be attributed to the increase in their acidity and or to the increase in their surface area. The activation energies, E_a for the oxides investigated were calculated from the plots of $\log k$ against $1/T$.

The E_a values obtained are given in table (2) from which it can be seen that the lowest activation energies is for the decomposition of 50 % ZrO_2 . This indicates that the acidic sites present on the oxides surface accelerate the decomposition rate of H_2O_2 according to the following mechanism.



Where A^+ are the acidic sites present on the surface.

Electrical conductivity may give a schematic model for the mechanism of semiconductivity in solid, containing OH groups. The electrical conductivity, σ of calcined samples ZrO_2 , SiO_2 and their mixture was measured as a function of temperature in the range 25–500°C. The results obtained are represented graphically by plotting in σ against $1/T$; Fig. (8) and all conductivity data are summarized in Table (3). There are two distinct lines (I and II).

The first portion (I) may be represent the extrinsic conductivity and the second (II) portion represents the intrinsical domain of conductivity.

The conductivity values of ZrO_2 lie in the range of semiconductors. For pure ZrO_2 sample and for those with 90 mole % respectively, a thermoelectric effect investigated at room temperature was measured. It showed that the charge carriers are of electronic nature. The temperature T_b at which the break in the distinct lines appear, shifts to a higher temperature with increasing ZrO_2 ratio. This can be attributed to the decrease in the concentration of impurities. Table (3) shows that the minimum conductivity attributed to the pure SiO_2 .

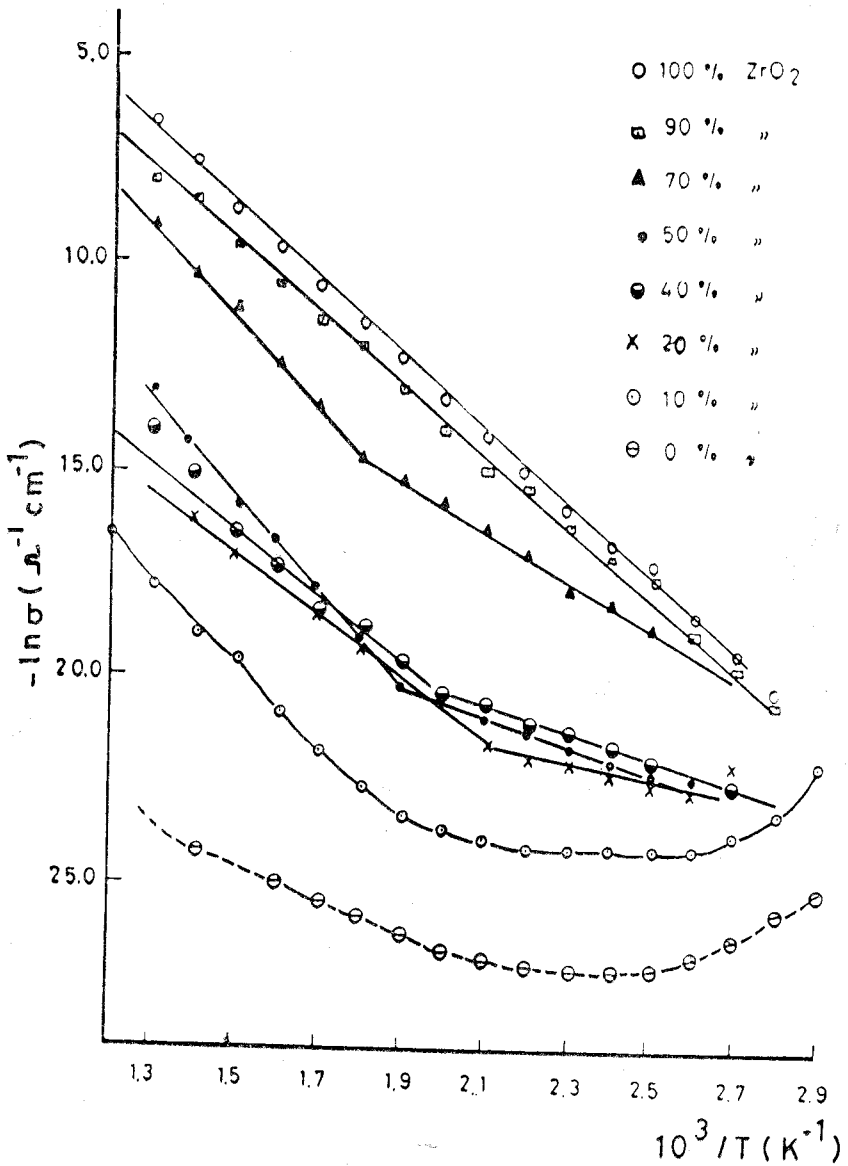


Fig. 8. The Effect of Temperature on The Electrical Conductivity of The Mixed Oxides $\text{SiO}_2 \cdot x\text{H}_2\text{O} - \text{ZrO}_2$ Calcined at 750°C .

Table 3. Electrical conductivity data of SiO₂-ZrO₂ system.

Composition samples	Tb(°C)	σ^*	E* kJ mol ⁻¹	r
SiO ₂	—	—	56.62	0.9999
I	—	—	—	—
II	200	4.598 ⁻¹⁰	33.458	0.9891
III	220	3.7559 ⁻⁹	30.5073	0.986
IV	250	1.526940 ⁻⁹	21.9689	0.9891
V	270	4.12924 ⁻⁷	40.692	0.999 ⁻
VI	—	—	62.629	0.9985 ⁻
ZrO ₂	—	—	2.31149	0.995

σ^* = Electrical conductivity in ($\Omega^{-1} \text{ cm}^{-1}$).

Tb = Temperature at which break in conductivity occurs.

REFERENCES

1. M. MILLER., Phys. Rev., 60, 890 (1941).
2. A.R. HUSTON., J. Chem. Solid, 8, 467 (1959).
3. N.F. MOTT. and R.V. GUNNEY., "Electronic Process in Ionic Crystal" Ino Publisher, N.Y. (1964).
4. S. FUJTSU., K. KOIMOTO. and H. YAMAGIDA., "Solid State Ionic" 18, 1146 (1986).
5. K.H. KIM and J.S. CHOI., J. PHYS., Chem. Solids 45, 1265 (1984).
6. J.S. CHOI and K.H. KIN., J. Phys. Chem. 80, (1976).
7. H. GRUBER and E. KROUTZ Zeit. Fur, Met., 74, 203 (1986).
8. HELMUT KNOZINGER, in "Advances in Catalysis", Editors D.D. ELEY., HERMAN PINES. and PAUL B., Weisl, Volume 25, pp 184 (1976), Pub. Academic Press, New York., London.
9. T. SUMIYOSHI., K. TANABE., H.H. ATTORI., Bull. Jpn. Petrol, Inst., 17, 65 (1975).
10. V.A. DZISKO., Proc. Intern. Congr. Catalysis, 3rd, Amsterdam, 1, 19 (1964).
11. Y. IZUMI. and T. SHIBA., Bull. Chem. Soc. Japan., 37, 1797 (1964).
12. T. KAWAGUCHI, S., HAREGAWA, K.K. ASEDA. and S. KURITA., Shashin (Japanese), 9, 112 (1968).
13. IDEM. Z., Anonrg. Allg. (LpZ), 38, 400 (1973).
14. V. MUCKA., Collec. Czech, Chem. Commun. 46, 876 (1981).
15. Idem. Ibid 1, 49 (1984).
16. O. JOHNSON., J. Phys. Chem. 59, 827 (1955).
17. K.B. KEATING., M. MATSUMOTO. and KOBOYASHI, J., Catal. 21, 48 (1971).
18. M.A. MOUSA., E.A. GOMMAA., A.A. EL. KHOULY., Mater Chem. Phys. 11, 433 (1984).

19. R.S. Mc DONALDL., *J. Phys., Chem.*, 62, 1168 (1958).
20. E. NARUKO and H. KOGYO., *J. Phys. Chem.*, 67, 2019 (1964).
21. H.J.E. MELEUS. and A.C. JONES, *J. Phys., Chem.*, 63, 172 (1959).
22. J.B. PERI, *J. Phy. Chem*, 70, 2937 (1966).
23. A.V. KISELEV., *Structure and Properties of Pourous materials, Colston papers, Vol. 10* (D.H. Everett and F.S. Stone Eds.) Bullerowrth, London, P. 195 (1958).
24. H.J. EMELEUS, and A.C. JONES, *J. Phys. Chem.*, 63, 172 (1959).
25. J.B. PERI, *J. Phys. Chem.*, 70, 2937 (1966).